

Numerical investigation of flow around fixed cylinder at
 $Re=3900$: Study of spanwise length optimization



Author

Haider Ali

Reg. Number 00000277811

Supervisor

Dr. Niaz Bahadur Khan

SCHOOL OF MECHANICAL & MANUFACTURING ENGINEERING

NATIONAL UNIVERSITY OF SCIENCES AND TECHNOLOGY

ISLAMABAD

July 2021

Numerical investigation of flow around fixed cylinder at
Re=3900: Study of spanwise length optimization

Author

Haider Ali

Reg. Number 00000277811

A thesis submitted in partial fulfillment of the requirements for the degree of
MS Mechanical Engineering

Thesis Supervisor:

Dr. Niaz Bahadur Khan

Thesis Supervisor's Signature: _____

SCHOOL OF MECHANICAL & MANUFACTURING ENGINEERING
NATIONAL UNIVERSITY OF SCIENCES AND TECHNOLOGY,
ISLAMABAD

June 2021

THESIS ACCEPTANCE CERTIFICATE

It is certified that the final copy of MS/MPhil thesis Written by Mr. Haider Ali (Reg. No: 00000277811), of SMME (School of Mechanical and Manufacturing Engineering) has been vetted by undersigned, found complete in all respects as per NUST Statutes/ Regulations, is free of plagiarism, errors and mistakes and is accepted as partial fulfillment for award of MS/MPhil Degree. It is also validated that any essential changes suggested by GEC members have been included in this dissertation.

Signature: _____

Name of the supervisor: Dr. Niaz Bahadur Khan

Dated: _____

Signature (HOD): _____

Dated: _____

Signature (Principal): _____

Dated: _____

MASTER THESIS WORK

We are hereby recommended that the dissertation prepared under our supervision by: Haider Ali, (Reg. No 00000277811) Titled: “Numerical investigation of flow around fixed cylinder at $Re=3900$: Study of spanwise length optimization” be accepted in partial fulfillment of the requirements for the award of MS Mechanical Engineering degree with (.....) grade.

Examination Committee Members

1. Name: **Dr. Muhammad Sajid**

Signature: _____

2. Name: **Dr. Mian Ashfaq Ali**

Signature: _____

3. Name: **Dr. Emad ud din**

Signature: _____

Supervisor's name: **Dr. Niaz Bahadur Khan**

Signature: _____

Date: _____

Date: _____

Head of Department

COUNTERSIGNED

Dean/principal

Date: _____

Declaration

I certify that this research work titled “Numerical investigation of flow around fixed cylinder at $Re=3900$: Study of spanwise length optimization” is my own work. The work has not been submitted to anyone else for review. The content that has been used obtained from other published resources. It has been recognised / referred in the right manner.

Student Signature

Haider Ali

2018-NUST-MS-ME-00000277811

Plagiarism certificate (Turnitin Report)

Plagiarism has been checked in this thesis. Attached is a Turnitin report that has been approved by the supervisor.

Student Signature

Haider Ali

2018-NUST-MS-ME-00000277811

Signature of the supervisor

Copyright statement

- The student author retains the copyright in the text of this thesis. Copies (by any process) either in full, or of extracts, may be made only in accordance with instructions given by the author and lodged in the Library of NUST School of Mechanical & Manufacturing Engineering (SMME). The Librarian can provide more information. This page must be included in any copies made. Further copies (by any process) may not be made without the permission (in writing) of the author.
- The ownership of any intellectual property rights which may be described in this thesis is vested in NUST School of Mechanical & Manufacturing Engineering, subject to any prior agreement to the contrary, and may not be made available for use by third parties without the written permission of the SMME, which will prescribe the terms and conditions of any such agreement.
- The Library of NUST School of Mechanical & Manufacturing Engineering, Islamabad, has more information on the conditions under which disclosures and exploitation may occur.

Acknowledgement

I am grateful to my Creator ALLAH for guiding me through every step of this project and for every new notion You implanted in my mind to help me enhance it. Indeed, I could have done nothing without your priceless help and guidance. Whoever helped me throughout the course of my thesis, whether my parents or any other individual was your will, so indeed none be worthy of praise but you.

I am grateful to my loving parents, who reared me from the time I was unable to walk and have continued to support me in every aspect of my life. Especially my father who is the real boss of my life. He has planned my life quite efficiently and teaches me to do hard work whatever the circumstances are.

I am very thankful to my research supervisor Dr. Niaz Bahadur khan for his help throughout my thesis research and for the motivation and determination he gave me. He cares so much about any of his student's work and responds to queries and question so promptly.

I would also like to express my gratitude to Dr. Emad ud din for his unwavering support and collaboration. He always had an answer for me when I was stuck on something. I would not have been able to finish my thesis without his assistance. Throughout the thesis, I appreciate his patience and help.

Special thanks to Mr. Muhammad Sajid and Mr. Mian Ashfaq Ali for being on my thesis guidance.

Finally, I would like to express my gratitude to all the individuals who have rendered valuable assistance to my study.

Dedicated to my family and friends, whose love, admiration and collaboration helped me achieve this fantastic goal.

Abstract

One of the most fundamental engineering problems is flow around a circular cylinder, which has been substantially studied with applications such as heat exchangers, marine cables, chimneys, and offshore supporting feet. From a theoretical standpoint, flow around a circular cylinder exhibits many important fluid dynamics phenomena, including turbulent transformation, vortex shedding and flow separation. Despite significant numerical and experimental research [1], [2] and [3-6], flow around a circular cylinder is still a difficult problem in fluid mechanics, prompting ongoing research to better understand the cylinder's complex unsteady flow dynamics. Large Eddy Simulation (LES) coupled to Smagorinsky and dynamic sub grid scale models were used to investigate transitional flow past a circular cylinder in the lower subcritical regime ($Re = 3900$). Even though many researchers have looked into this issue, there is still a disparity in the results, especially when it comes to calculating the separation angle, recirculation length and flow characteristics in the wake region behind the cylinder. Furthermore, the impact of spanwise length and grid resolution in the spanwise direction should be addressed. This research examines previous research and conducts studies in accordance with literature guidelines. The influence of change in spanwise length ($0.5D$, $1D$, $2D$, πD , $4D$ and $8D$), mesh resolution in the spanwise direction (ranging from 1 to 80 elements) on separation angle, recirculation length and wake characteristics is examined. Within 10 diameters, the wake behind the cylinder is inspected. This study revealed optimized spanwise length and mesh design and concluded that mesh resolution in the spanwise direction is a more important factor for good results than spanwise length.

Keywords:

$Re=3900$, spanwise length, effect of spanwise resolution, numerical simulations, LES model, flow around cylinder

Table of Contents

THESIS ACCEPTANCE CERTIFICATE	3
Declaration	i
Plagiarism certificate (Turnitin Report).....	ii
Copyright statement	iii
Acknowledgement.....	iv
Abstract	vi
List of Figures	viii
List of Tables.....	viii
List of Graphs.....	viii
CHAPTER 1: Introduction	1
1.1 Background	1
1.2 Literature Review	2
1.3 Problem Statement:	6
1.4 Objectives:.....	7
CHAPTER 2: Numerical approach	8
2.1 Numerical model	8
2.2 Flow around cylinder at Reynolds number = 3900.....	10
CHAPTER 3: Methodology	11
3.1 Computational domains and boundary conditions.....	12
3.2 Ansys/Fluent.....	15
3.2.1 Computer Aided Design Model.....	15
3.2.2 Mesh:	16
CHAPTER 4: Results and Discussions	19
CHAPTER 5: Conclusions	28
Future Recommendations	28
References	29

List of Figures

Figure 1. Computational domain and boundary conditions
Figure 2. 3D view of cylinder with boundary conditions
Figure 3. Mesh design.....
Figure 4. (a) Mesh closeup view in spanwise direction.....
Figure 4. (b) Mesh closeup view near cylinder
Figure 5. Vertical profiles and centerline sketch behind the cylinder.....

List of Tables

Table 1. Mesh details and boundary conditions used in previous studies by other researchers
Table 2. Input boundary conditions.....
Table 3. Results comparison with variation of grids in spanwise direction.....
Table 4. Results comparison with variation of grids in spanwise direction.....
Table 5: At $Re=3900$, comparison between numerical and experimental results.....

List of Graphs

Graph 1. Coefficient of pressure vs Θ
Graph 2. Mean stream velocity at centerline, behind the cylinder.....
Graph 3. Comparison of mean stream velocity profiles of flow over cylinder at $X/D=1$, $X/D=3$, $X/D=5$ for present study and other numerical and experimental results.....
Graph 4. Comparison of mean crossflow velocity profiles of flow over cylinder at $X/D=1$, $X/D=3$, $X/5$ for present study and other numerical and experimental results.....

CHAPTER 1: Introduction

1.1 Background

Flow around cylindrical structures is a typical phenomenon to examine in today's world due to wide range of applications in engineering field such as aerodynamics, bridges, skyscrapers, nuclear reactors, chimney stackers, and wind turbines, among others. In 1940, Tacoma narrow bridge collapsed. It is because of the vortex induced vibrational effects on the bridge. Vibrations induced by a vortex are extremely harmful and catastrophic in nature. Researchers and designers are analyzing the designs and dynamics of flow over cylinders empirically, experimentally, or numerically in response to the Tacoma bridge incident. They are first working on the optimum design and failure mode analysis of structures utilizing computer aided design (CAD) and analysis (ANSYS, MATLAB) tools, instead of constructing expensive buildings using labor. They are now concentrating significantly more on high-skilled workers and high-quality experimental techniques. This thing alters the traditional method of building by hand without any precautions or analysis. Researchers' attention has shifted to studying numerically rather than relying solely on experimental investigations as a result of significant advances in the computational fluid dynamics discipline. Rather than its basic geometry, the fundamental reason for studying flow over a cylinder both experimentally and numerically is owing to its unpredictable and complex flows. Because of the intricacy of flow over the cylinder, studying environmental and natural flow conditions and testing computing programmes on this analysis will be highly fascinating. It is also a good starter to study even more complex geometries and flows.

Because vortex induced vibrations are dangerous, they must affect a wide range of technical applications, including underwater pipelines, submarines, skyscrapers, bridges, and electricity transmission lines. Many businesses that are highly dependent on vortex induced vibrations, such as marine cables, drilling risers, buildings, constructions in flowing water, catenaries, and so on, can be observed with a cylinder enduring vortex induced vibrations. This phenomenon is much dependent on computational domains and boundary conditions of the bluff body.

Previous data will be validated as a result of the study in order to better understand the variation in results and other features of flow by changing spanwise mesh resolution and spanwise length. In terms of mesh type and computational domain size, previous research is also examined and validated.

1.2 Literature Review

Flow over cylinder is studied by many researchers in past years as shown in past review papers.

Williamson [7] stated that von Karman vortex structures appear at Reynolds number=49. When Reynolds number rises, it will result in laminar flow transitioning to turbulent characteristics of flow. Turbulent flow transition is easily observed in shear layer at Reynolds numbers ranging from 300 to 200,000. At $Re=3900$, flow around a cylinder enters the lower subcritical region, where the boundary layer is laminar, and the shear layer transitions in the wake region behind the cylinder. The region next to the cylinder then becomes highly complex because of the change in the segregating shear layer and the shedding of massive vortices. That is why it is of particular interest to past researchers because of its complexity of nature over the wake of cylinder. In boundary layer, shear layer or in wake, this transition can occur. Bearman [8], Breuer [9] and Sarpkaya [10] extensively performed numerical studies on flow over cylinder and cleared my obstacles regarding to understand the flow characteristics. Breuer [9] comes up with good and satisfactory results in comparison with the experimental data after performing an investigation study on flow over cylinder using Large eddy simulation technique with $Re=3900$ for flow over cylinder. Much of the analytical data was gathered for 100 D/U time units or 22 vortex-shedding cycles, but the author addressed the importance of keeping data for a long time. Breuer [9] used a Smagorinsky model to compute a low value of recirculation length ranging from 1.0 to 1.1 and a dynamic model with the same number of vortex-shedding period data to compute a high value of recirculation length ranging from 1.1 to 1.4. The author also came to the conclusion that near-wall and subgrid-scale (SGS) models play important roles in modelling. Breuer [9] demonstrated that the Strouhal number is not a particularly sensitive parameter, and that its precise measurement of Strouhal number does not guarantee high-quality performance and results. Breuer [9] also came to the conclusion that central schemes with second- or fourth-order precision produce better performance and results, whereas the upwind scheme is unsuitable and not recommended. As opposed to the dynamic Smagorinsky model, the traditional Smagorinsky model highly predicted the importance of drag coefficient and separation angle. When using large eddy simulations (LES) for the flow query, Breuer [9] emphasized the importance of spanwise resolution. Tremblay et al [11] studied the effects of the SGS model and also grid resolution on large eddy simulations using technique known as Cartesian grid. The length of recirculation period and profiles of mean could not be reliably predicted in this analysis. Lysenko [12] used analysis software (OpenFOAM) in order to investigate the flow around cylinder using a dynamic sub-grid scale k-equation SGS model and the large eddy simulations model. Lysenko et al

[13] used large eddy simulations with a blended central-difference scheme to calculate the flow around a cylinder at Reynolds number = 20,000. Parnaudeau et al [14] used LES with a high order scheme to simulate a flow over cylinder. The numerical analysis of power spectra and turbulence statistics up to 10 D. The authors came to the conclusion that the precision with which the recirculation duration is predicted is the determining factor in the agreement across numerical and experimental performance. At $Re = 3900$ and 10,000, Dong [15] used PIV experimental calculation and DNS simulations to test Reynolds number's impact on shear instability and statistics of wake. Norberg [16] looked at aspect ratio influence on Strouhal number and also mean base suction coefficient calculated at the mid-span location in another experiment. Wissink and Rodi [17], Dong et al [15], uses DNS method in order to investigate flow over cylinder. This numerical method is highly precise and gives detailed and proper insights of characteristics of flow. But its cost on computation is high even when operated at moderated Reynolds number, which makes it very difficult to use for problems when Reynolds number is high. Several laboratory experiments using various methods examined the wake behind the cylinder (up to 10D of cylinder).

Since many practical and engineering applications are found in these flow regimes, the reviews conducted by Bearman [8], Norberg [2] and Sarpkaya [10] revealed that response of the amplitude is particularly vulnerable to Reynolds number, which is well known at low Reynolds numbers. However, further research is necessary to clarify its impact at high subcritical values and then across the critical range. In the case of turbulent flow, large eddy simulation, Reynolds averaged numerical simulation, and direct numerical simulations are commonly used. RANS is a new technique that is gaining popularity due to its low computational cost and reasonable performance. Ong and Wallace [18] inspected the velocity profile in the wake region behind the cylinder from 3D to 10D and verified the precision of X-ray results. There are few studies on VIV in circular cylinders at higher Reynolds Numbers, while low Re and low mass ratios have been studied extensively.

Zhao [19] investigated the vortex induced vibrations in the Reynolds numbers range of $Re = 150$ to 1000 by using 3-dimensional Navier-Stokes equations. These studies revealed that 2D Navier-Stokes is not appropriate for solving VIV in turbulent flows. Using the 2D (2 Dimensional) RANS code, on the other hand, yielded consistent results. Niaz bahadur khan [4] used LES code and the Smagorinsky—Lilly subgrid-scale model to identify the effect of spanwise length and mesh resolution on measuring recirculation length and angle of separation around a fixed structure at Reynolds number = 3900. In comparison to other simulations and experimental studies, the drag coefficient, Strouhal number, separation angle, and length of recirculation are all really well obtained. The

estimation of the recirculation length, wake characteristics of flow and angle of separation behind the cylinder is greatly influenced by near field grids spanwise resolution. This study also found that the coarse mesh leads to an overpriced drag value, a delay in distance angle (angle of separation), an undervalued strouhal number and a short recirculation duration in the span direction. The findings of this analysis are in line with the experimental findings, and a better profile was expected than past simulation studies. In the wake near the cylinder, experimental results show that aspect ratio has a major impact, while numerical simulations are mainly dependent on density of mesh in spanwise direction. The instantaneous field gained via steady state flow by using k- ω model was used as an initial field for the large eddy simulation run, resulting in a decrease in simulation time and statistical convergence performance. Niaz[4] also concluded that mesh density is an important parameter for accuracy of results . Niaz[4] concluded that analysis at $Re= 3900$ is not just 2-Dimensional case, and the resolution of mesh in spanwise domain has a substantial impact on the outcomes. In order to find For a better understanding of the vortex induced vibration phenomenon, Khalak and Williamson [20] conducted experiments at low mass ratios in the Reynolds number range of $Re = 1,700$ to $12,000$. Numerical analyses were performed by Guilmineau and Queutey [21], Pan and Cui [22], and Wei Li [22] to confirm their findings with experimental results obtained by Khalak and Williamson [20]. Despite being able to predict the vortex-shedding mode and transition between different modes, their research was unable to compute the maximum amplitude response. To confirm their findings with experimental work done by Hover [23], Nguyen V-T and Nguyen HH [24] used detached-eddy simulation (DES) [a hybrid of RANS and LES] at low mass ratio and high Reynolds number. It also showed a high level of agreement with experimental findings. At high values of Reynolds number (10^4) and low values of mass ratio, Niaz et al. [5] conducted a numerical analysis using the computationally less costly RANS shear-stress transport (SST) k-w turbulent model, and the findings agreed well with the scientific investigations and three-dimensional DES.

The mass ratio of a flow over the bluff body is a critical parameter that influences flow characteristics and the Vortex induced vibration phenomenon. Williamson and Govardhan [25] conducted a detailed analysis of the impact of damping and mass ratios in a review report. Their analysis revealed how the mass ratio affects the dominant frequency in synchronizing conditions, maximum amplitude reaction in the top and bottom branches, and the upper limit of U_r in the synchronizing area. Using direct numerical simulations, Dong [15] and Me [26] studied characteristics of mean flow and energy spectrum up to 10-Diameters . Ramzi [27] investigated the Vortex induced vibration phenomenon and

dynamic responses in the direction of crosswise flow using a short rigid cylinder. At a moderate to high values of Reynolds number, Rajani [28] investigated the restriction of URANS in measuring drag forces, skin friction coefficients and mean pressure coefficients.

Zhang [29] investigated the effects of infinite and finite circular cylinders on mechanics of flow, concluding that a finite cylinder with a free end has a major effect on the wake field. Frohlich [30] used LES with specialized code to investigate the impact of structured and unstructured grids at Reynolds number=3900 and 140,000. In the shear layer of transformation, Moin and kravchenko [31] concentrated on grid resolution. Inadequate grid resolution can cause early change in the shear layers, resulting in erroneous results. Rodi and wissink [17, 32] used direct numerical simulations in order to run a series of numerical simulations at Reynolds number= 3300 and then compared the findings to experimental studies at Reynolds number= 3900. The roll-up of the splitting shear layer, which transforms to turbulence, was observed. Even at low Reynolds numbers, direct numerical simulations is costly and provides accurate and reliable performance. The high computational cost of DNS for moderate and high Reynolds numbers is a big stumbling block. In a subcritical regime, flow around cylinder is mainly studied using large eddy simulations (smagorinsky model) with fixed coefficient but without model, and with a dynamic model due to the deficiencies in the URANS method and the greater computational cost of direct numerical simulations. Townsend [33] studied the wake characteristic in a fully established field, going beyond 10D. Yamada [34] investigated Reynold's shear stress, mean velocities and velocity diffusion in the $x/D= 30.5$ to 475 area far away from the cylinder. Norberg [35] looked at some of the other subcritical experiments that had been done. On the computational side, the flow around cylinder has primarily been studied using the URANS, DNS, and massive LES. Franke and Frank [36] used a cell-centered volume code to perform a sequence of large eddy simulation at Reynolds number = 3900. Short-time averaging data (with 10-21 vortex-shedding cycles) result in a short recirculation length, according to the report. High values of recirculation duration and base pressure are obtained by increasing time averaging to 42 averaging cycles. However, the authors point out that the research is insufficient to arrive at a statistically converged solution. Kravchenko and Moin [31] used large eddy simulations and a high-order precise numerical model which is based on B-splines to investigate the flow around a cylinder at Reynolds number = 3900. They came to the conclusion that low mesh resolution in the shear layer causes limited recirculation lengths values and vice versa. At Reynolds number = 5800, Shao and Zhang [37] compared the Reynolds-averaged Navier–Stokes (RANS) and large eddy simulation results (same sub-critical regime). The momentum equations were

solved using a second-order upwind scheme and bounded central differencing scheme. A SIMPLE algorithm was used for pressure-velocity coupling. Over 15 vortex-shedding periods, Shao and Zhang [37] calculated time-average statistics for flow and turbulence quantities. Young and Ooi [38] used LES and the Smagorinsky SGS model to numerically simulate the flow over cylinder at Reynolds number = 3900. The simulation was run for 60 non-dimensional time steps before the time statistical data were collected to ensure that the flow was free of initial conditions and completely formed. The data was collected for 30 vortex-shedding periods. At low reduced velocities, the vortex induced vibration lock-in phenomenon occurs earlier in the streamwise direction than in the transverse direction, so the Vortex induced vibration amplitude response is higher in the streamwise direction than in the transverse direction. Zhipeng feng [39] uses LES model of OpenFOAM is used to measure the steady flow over cylinder at Reynolds number=3900. The lift and drag coefficients, as well as distribution of pressure over cylinder, the velocity profiles and Reynold's stress distribution in the wake field, and angle of separation and recirculation length, are all predicted. The aim of this paper is to use a benchmark problem to compare the performance of the Open FOAM sub grid model quantitatively, as well as to address some key factors that affect predictive performance. A sircar [40] run non-isothermal LES of flow over heated cylinder at Reynolds number = 3900 in order to test flow physics in the wake area and build a basis upon which future heat flux wall models (both for wall-modeled LES and other lower fidelity models) can be constructed for mathematical closure of the energy equation (both for wall-modeled LES and other lower fidelity models). Because large-scale experimental and numerical data is readily available, Reynolds number= 3900 is a significant topic to examine the competence and effectiveness of computational techniques and tools in researching and estimating the characteristics of flow around the cylinder. Because of numerous flaws in previous studies, further numerical and experimental studies of the flow characteristics over cylinder are needed. In terms of mesh type and computation size of domain, previous studies are also examined and reviewed.

1.3 Problem Statement:

The aim of this project is to check the change in numerical results by changing spanwise length of cylinder and by changing mesh resolutions in the spanwise direction. Although a lot of work is done in past, but there is still some gap in research of below than πD spanwise lengths.

1.4 Objectives:

This research work includes following objectives:

- To investigate optimum spanwise length in order to optimize computational time and cost.
- To investigate optimum mesh design.
- To investigate the effects of changing spanwise length on the wake characteristics of flow.
- To investigate the effects of changing spanwise length. on recirculation length, drag coefficient, angle of separation and Strouhal number.
- To investigate the effects of changing spanwise resolution of mesh on recirculation length, drag coefficient, angle of separation and Strouhal number.

CHAPTER 2: Numerical approach

This chapter demonstrates the numerical approach used to numerically investigate the flow over cylinder in order to check the change in parameters and results with the variation of change and spanwise length and resolution of mesh in the spanwise direction. Using a large eddy simulation (LES) model, all simulations are run at a subcritical Reynold's Number of 3900.

2.1 Numerical model

The Large eddy simulation (LES) model has great potential to model flow at high values of Reynolds number while also addressing 3D bluff body flow at a lower cost. Massive turbulence is specifically simulated in this space filtering process, and SGS turbulence is developed and modelled. The LES method was chosen for this analysis because it was found to be a more promising and effective tool for turbulent flow simulations [41]. Only the effect of small eddies must be modelled using a sub-grid scale model in LES, while the large energy-carrying eddies must be computed directly. Small eddies are more general, unpredictable, monocultural, and isotropic, making the construction of suitable models easier. The distinction between small and large scales is made using delta filter (Δ) function.

In this current study, the fluid flow past a cylinder is considered an incompressible, two dimensional and unsteady flow. The unsteady Reynolds–Averaged–Navier–Stokes (RANS) equations can be written as:

$$\frac{\partial \bar{u}_i}{\partial x} = 0 \quad (1)$$

$$\frac{\partial \bar{u}_i}{\partial t} + \frac{\partial (\bar{u}_i \bar{u}_j)}{\partial x_j} = -\frac{1}{\rho} \left(\frac{\partial \bar{p}}{\partial x_i} \right) + \nu \left(\frac{\partial^2 \bar{u}_i}{\partial x_i \partial x_j} \right) - \frac{\partial \tau_{ij}}{\partial x_i} \quad (2)$$

where τ_{ii} , p and ρ are, respectively, the non-resolvable SGS, pressure and density of fluid. The velocity variable is shown by u_i and u_j in i and j directions respectively, and the space filtered quantities are shown by the over-bar on velocity variable. for example, u and v are velocity in the x and y directions, respectively; u_i and u_j are fluctuation velocity components in the i and j directions, respectively. Furthermore, x_i and x_j are Cartesian coordinates in the i and j directions.

$$\tau_{ij} = \overline{u_i u_j} - \bar{u}_i \bar{u}_j \quad (3)$$

In above equation, τ_{ij} is called sub-grid scale term. Sub-grid scale (SGS) stresses are modelled in ANSYS Fluent using the popular Boussinesq hypothesis [42]. The Smagorinsky model is the most widely used in LES [43].

$$\tau_{ij} - \frac{1}{3}\tau_{kk} = -2 \cdot \nu_{SGS} \cdot \bar{S}_{ij} = \nu_{SGS} \cdot \left| \frac{\partial \bar{u}_i}{\partial x_j} + \frac{\partial \bar{u}_j}{\partial x_i} \right| \quad (4)$$

$$\nu_{SGS} = (C_s \Delta)^2 |\bar{S}| \quad (5)$$

In above equation, term ν_{SGS} , C_s and \bar{S} represents sub-grid scale eddy viscosity, smagorinsky constant and strain rate tensor respectively. C_s is taken as 0.2 for homogenous turbulent flows by smagorinsky [43]. Lilly [44] and germane [45] established a methodology for calculating the C_s value which is dynamically relying on the input data. The Ferziger and peric [46] thesis study contains a full mathematical description of the dynamic SGS model.

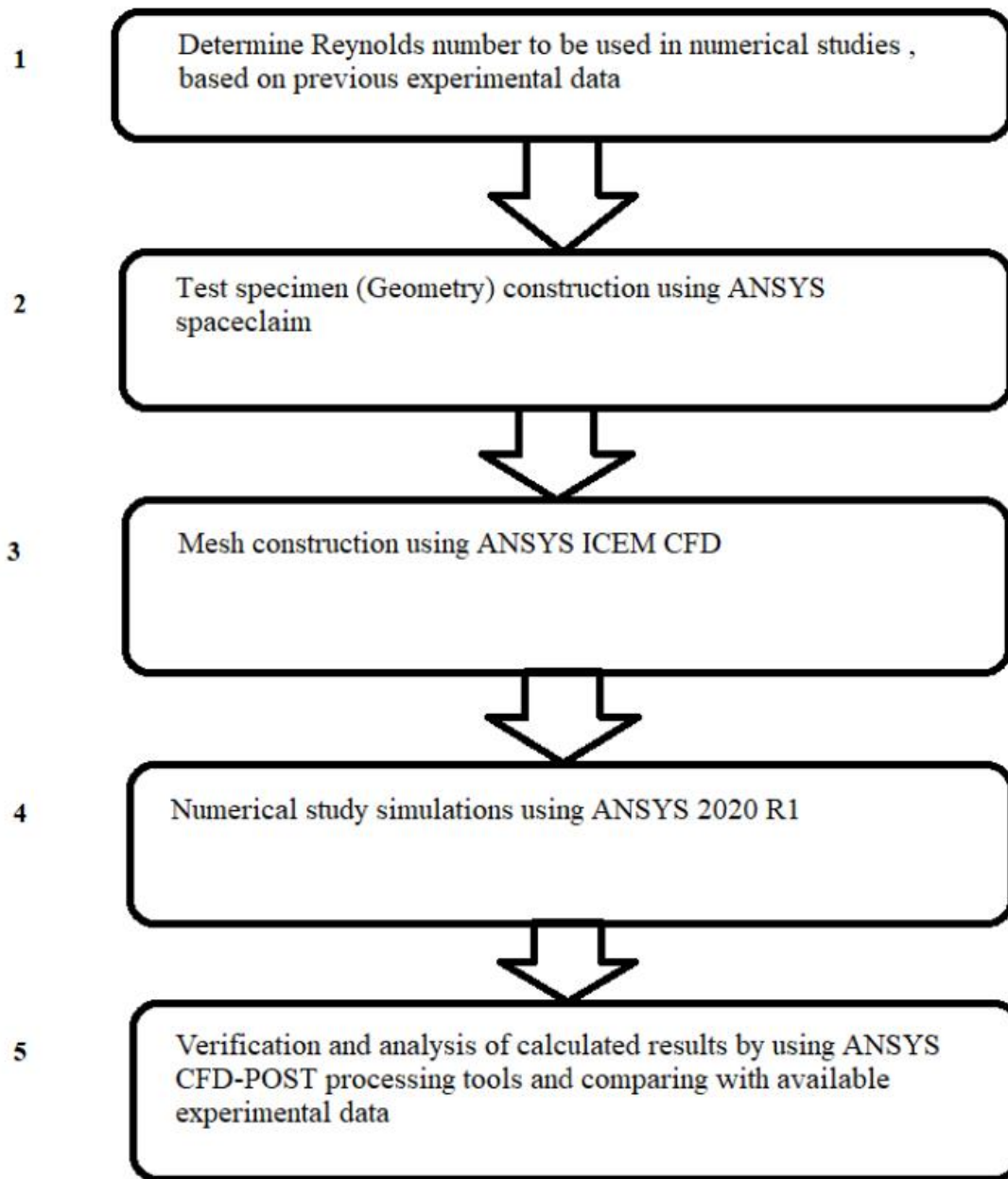
The effects of turbulence are expressed in this model by eddy viscosity, which is based on the Boussinesq hypothesis. The SST $k-\omega$ turbulence model was proposed by Menter [47] which is an improved version of the standard $k-\omega$ model combining the pros of both $k-w$ model and k -epsilon model. In comparison to direct numerical simulation (DNS) and large eddy simulation (LES), numerical simulation using the SST $k-\omega$ model consumes much less computational cost. The LES model is combined with the Smagorinsky–Lilly SGS model coupled with dynamic stress activated in this analysis. A pressure-based solver “SIMPLE” has been assigned to the simulation. To obtain a consistent solution, a second-order temporal discretization scheme for simulations was then used. For Large Eddy Simulation model, bounded second order scheme is applied in the momentum equations in order to capture better results, whereas bounded second-order implicit transient formulation was used. In comparison to the second-order implicit scheme, bounded second-order implicit is thought to be more stable and accurate [48]. The LES simulation must be performed for enough time to become completely independent of the initial conditions and to evaluate the flow field statistics. All the numerical studies began with the steady-state of flow using the $k-\omega$ model. After the steady-state RANS simulation has developed and converged, the instantaneous field was used as an initial field for the LES run. These guidelines are suggested by ANSYS[48], Niaz[4] in order to reduce the computational time. After the simulation ran for 120 flow time seconds, data was sampled to confirm that the developed flow had reached a statistically steady state transient behavior.

2.2 Flow around cylinder at Reynolds number = 3900

The flow over cylinder at Reynolds number = 3900 was studied with resolution of grid in the spanwise domain, with the number of elements changing from 5 to 80. In the wake area, velocities profiles in streamwise and crossflow directions are analyzed at the centerline up to 10D. The separation angle (θ_s) is calculated from the stagnation point S on the cylinder's wall to the separation point (clockwise) on the cylinder's wall, where O is the origin. This point is known in theory as the point at which the boundary layer separates from the cylinder surface due to an adverse pressure gradient. The separation angle is calculated numerically by locating the point on the cylinder surface where skin friction coefficient or mean wall shear stress is minimum.

CHAPTER 3: Methodology

The literature review and numerical analysis were used in this research. Phase 1 is a literature review of experimental data, followed by steps 2 through 5. The aim of Step 1 in the figure of calculating Reynolds number is to ensure that the numerical calculation result is correct in past. There are several Reynolds numbers ranges for flow over cylinder, each with its own set of experimental phenomena. The turbulent Von Karman Vortex Street phenomenon was chosen to be simulated in this analysis, and it occurred in the Reynolds number range of 300 to 300,000. In this analysis, the Reynolds number is 3900. This phenomenon makes it difficult to determine which turbulence model in ANSYS Fluent (2020 R1) better captures the turbulent Von Karman Vortex Street phenomenon. In this phenomenon, the effect of time phase size variation on the curve of lift coefficient of the circular cylinder is also important to know. The construction of a test specimen of a circular cylinder using software called ANSYS spaceclaim is the second phase of this study (see figure). Different 3D test specimens are designed with variations in spanwise length and mesh resolutions, in order to capture the best and optimize results for flow over cylinder. Third phase of this numerical study (see fig) is mesh constructions for these different specimens using ANSYS ICEM CFD tools. To achieve the best results, mesh construction is done with care. The fourth phase of this numerical investigation (see figure) entails importing meshes into Fluent in order to numerically simulate them and record the results. The fifth and final stage of this numerical investigation is post-processing. All numerical data is validated cross-checked against previously collected experimental data.



3.1 Computational domains and boundary conditions

Fluid flow over cylinder is much dependent on flow domain size. In steady or unsteady state, computational domain size is the main parameter in affecting the results of flow over cylinder. The main thing in selecting domain size is that it must be enough large to overcome effects of boundary walls in flow over cylinder.

In past studies, size of the domain varies from 15D to 70D in crossflow (Y) and streamflow (X) directions.

Many past studies extracted results using circular and rectangular domains. For circular domains, O-Grid meshing is typically used in studies. Computational domain is then separated into several hybrid or structured meshed regions. To resolve the wake region and boundary layers, grid points are being clustered in wake region and over the cylinder. In past studies, range of crossflow (L_y) domain is usually minimum of $20D$ up to maximum of $80D$, while range of streamflow (L_x) domain is usually minimum of $20D$ up to maximum of $40D$. In several cases, mesh is design in such a way that it is parted into regions, where O-Grid meshing is surrounded over cylinder and remaining region will then meshed using structured method. Different sized domain being used in past studies in literature.

- for flow over cylinder, $30D \times 16D$ sized domain is being used by Shao [37].
- Numerical study is done in transverse direction with the $8D$ sized domain by Fang and Han [49].
- Numerical investigation of Large eddy Simulations of flow is performed using $25D \times 20D$ sized domain for flow over cylinder by Franke J, Frank W [36].
- Numerical investigation of large eddy simulation is performed using $40D \times 20D$ sized domain in streamwise and crosswise for flow over cylinder, respectively. Different spanwise lengths ($16D$, $8D$, $4D$) were used by Niaz bahadur khan [4].

In previous studies, πD is the most studied case in spanwise depth where D is the diameter of the cylinder. Researchers tested the spanwise length up to $10D$. it is concluded that by varying length in spanwise direction from $4D$ - $8D$, there is a very little bit of change in results. [17], [32].

There is only 1% influence on solution by increasing spanwise length beyond $4D$. [50].

In most of the past studies, vortices formation in wake regions effected by size of domain. That is why it is preferable to use domain of large sizes in order to avoid boundary conditions disturbance.

In order to minimize cylinder response effects, blockage ratio of 5% (cylinder diameter / domain width) is supposed to be suitable. [51], [52], [49].

Due to this reason computational domain of size $40D \times 20D$ (streamflow \times crossflow) respectively is being used in this study. Different spanwise lengths $8D$, $4D$, πD , $2D$, $1D$, $0.5D$ are tested in order to compare their parameters and difference in results.

Below table shows details of mesh size of domains available in literature and used in past.

<i>Researchers</i>	$N_T \times 10^6$	<i>Mesh type</i>	$L_x \times L_y$	L_z
[17]	62	O-Grid	25D×20D	4D-8D
[14]	45.8	Hybrid	20D×20D	πD
[11]	7.7	Hybrid	20D×20D	πD
[12]	5.76	O-type	50D	πD
[53]	13.5	Hybrid	32D×16D	4D
[54]	5.5	O-type	35D	πD
[49]	1.7	Hybrid	24D×8D	10D
[55]	6	Hybrid	30D×20D	4D
[56]	1.04	Hybrid	32D×16D	3.288D
[9]	1.74	O-type	30D	πD
[4]	2.031	Hybrid	40D×20D	4D
[4]	3.064	Hybrid	40D×20D	4D
[4]	4.063	Hybrid	40D×20D	8D

Table.1 Mesh details and boundary conditions used in previous studies by other researchers.

Flow parameters are highly influenced by aspect ratio. Therefore, boundary conditions are periodically assigned to bottom and top of the wall so they can reduce the effect of impact ratio on the numerical results. Left side inlet boundary of the domain is placed 10D from center of the cylinder. Right side outlet boundary of the domain is placed 30D from center of the cylinder. Lower and upper walls of this computational domain is 10D from center of the cylinder and are symmetric in nature. In spanwise direction, periodic boundaries are assigned with multiple spanwise lengths (8D, 4D, πD , 2D, 1D, 0.5D) respectively. Velocity at inlet is 0.6 m/s, which is on right side of domain, maintaining Reynolds number $Re=3900$ by keeping diameter of cylinder $D=0.1m$, viscosity $=0.000016$ kg/ms, density $=1.04$ kg/m³. Left side of flow domain is pressure outlet with average static pressure of zero pascals. At the outflow border, a static reference pressure of 0 Pa is applied on average. A symmetric wall condition is applied to both upper and lower walls of flow domain. To investigate the boundary layer separation

and vortex generation phenomenon, a No-slip condition is given to cylinder wall. The result of applying No-slip condition is that the velocity near the cylinder wall would be zero and moving away from the cylinder it will increase to the freestream velocity. Below figure gives information about computer aided design model and boundary conditions.

3.2 Ansys/Fluent

In order to simulate the numerical processes and concluding results for flow over cylinder, Ansys Fluent (software) is selected. This software has a wide range of physical modeling which are required to model the flow and turbulence. All the numerical steps to find results are taken in this Ansys Fluent (software), from design of domain to solution of fluid. Below is the explained steps and summary of the completed process:

3.2.1 Computer Aided Design Model

The CAD model for flow around cylinder is generated using design modular (Ansys Fluent).

For flow over the cylinder, all computer aided design models are completely constructed by using space claim (Ansys Fluent).

Below figure shows details of computer aided design model constructed for this numerical study.

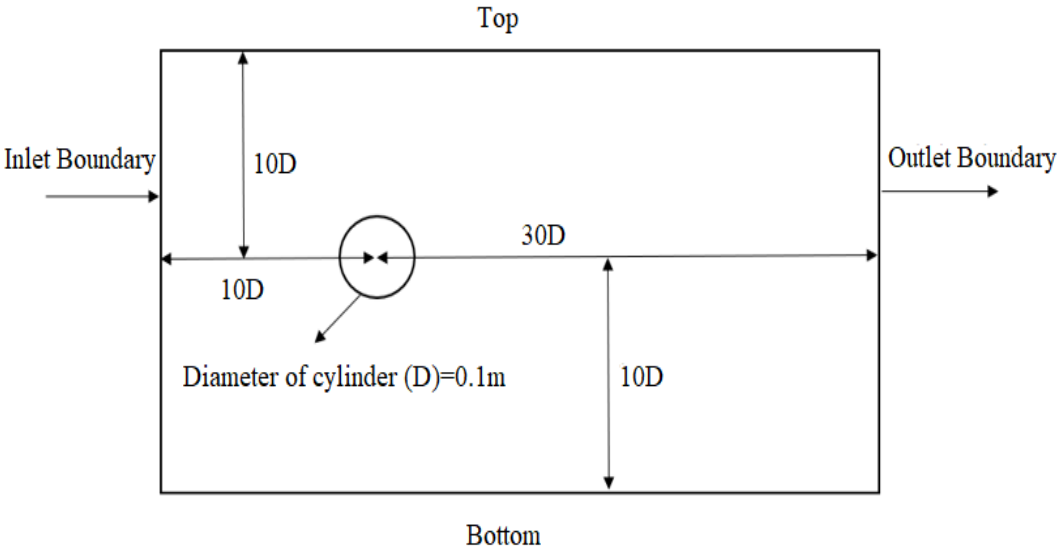


Figure 1: Computational domains and boundary conditions

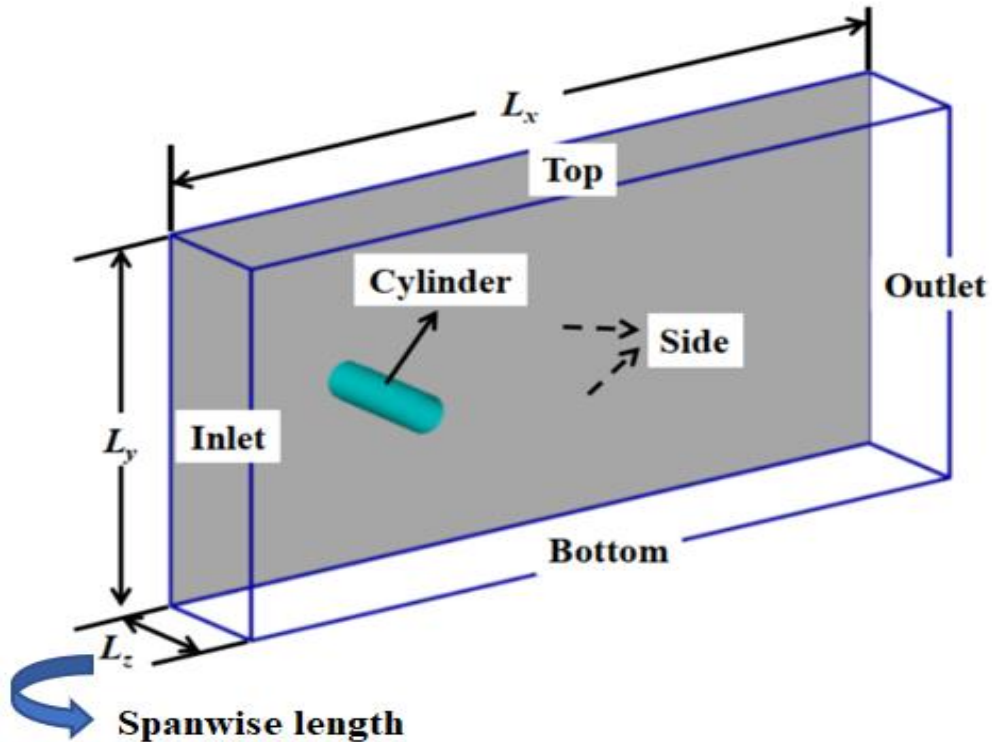


Figure 2: 3D view of cylinder with boundary conditions

3.2.2 Mesh:

In this numerical study, all the computer aided design models are then meshed by using ICEM CFD (Ansys Fluent) tools. All the meshes are designed using structured method of meshing and the computational domain is then divided into number of regions in such a way that they are O-Grid near the boundary wall of cylinder and then structured meshed away from the cylinder, in the computational domain. Rectangular domain is used in all numerical studies. The main and important characteristic of all the designed meshes is to secure the value of y^+ according to the numerical requirements. Flow over cylinder at Reynolds number=3900, produces turbulent eddies, because flow is in laminar separation regions in which separation occurs due to shear layers in wake of the cylinder. Therefore, regions over the cylinder will be meshed properly in order to ensure the resolution of boundary layers. First node is placed at 0.0002 or 0.002D in all numerical studies, in order to completely ensure y^+ less than unity.

Mesh development around the cylinder wall is very fine, whereas mesh development away from the cylinder wall is coarse. Below figures gives details of mesh and view near the wall of cylinder.

Y^+ value is known as the non-dimensional distance between first node of mesh and wall of cylinder, and it is very important for the accuracy of results and numerical values near the wake of the cylinder.

ANSYS [48] concluded that, value of y^+ must be smaller or equal to unity in order to ensure the proper resolutions of grids near the wall of cylinder. Grids are then made smooth, graded, symmetric and then divided into multiple zones in order to nullify the numerically occurred instabilities which results in poor quality of mesh. In current numerical study, y^+ less than 1 is maintained in all numerical cases. Multiple meshes are designed with different spanwise lengths and in some cases, study with different mesh resolution is performed in order to counter check the previous study results.

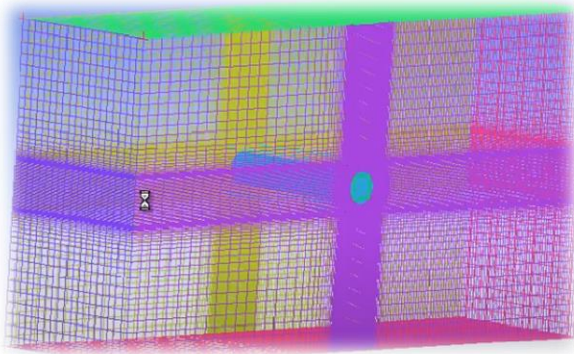


Figure 3: Mesh design.

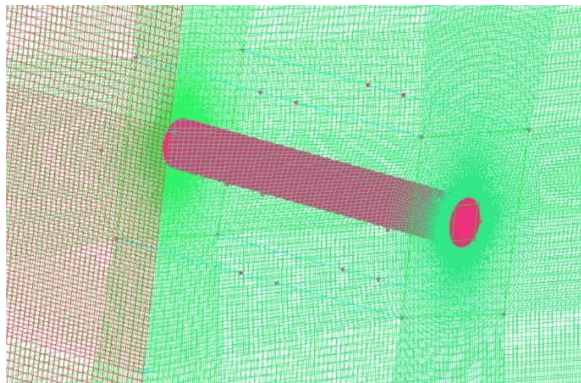


Figure 4: Mesh closeup view in spanwise direction.

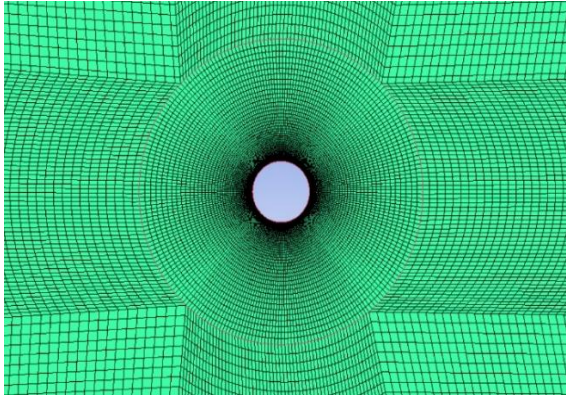


Figure 4. (b) Mesh closeup view over cylinder.

The details of all the input boundary conditions are shown in Table 2.

<i>Solver type /time</i>	<i>Pressure based /transient</i>
Models	LES (Smagorinsky-Lilly)
Materials	Air [Density (ρ) =1.04 kg/m ³] [Viscosity (ν) =1.6 e-05 kg/m-s]
Cell zone condition	Operating pressure=0
Boundary conditions (Inlet)	Velocity Inlet Velocity=0.6 m/s
Boundary conditions (Outlet)	Pressure outlet Pressure=transient tabular data
Solution method	Scheme = SIMPLE Formulation = Bounded second order implicit
Monitors	Drag coefficient, Lift coefficient
Solution initialization	Hybrid

Table 2: Input boundary conditions

CHAPTER 4: Results and Discussions

Table 3 displays case studies with a 2D spanwise length and mesh densities ranging from 2 to 0.05, with increasing elements from 1 to 40, respectively. Mesh density (M_z) is represented as spanwise direction (L_z) divided by the total number of elements in the spanwise direction (N_z). Case J which has only one element in spanwise direction with mesh density is equal to two, act as a 2-Dimensional case study. Since it is not able to accurately capture the flow characteristics. The value of the drag coefficient was overestimated in this situation, while the value of the Strouhal number was underestimated. It is observed that the solution is then converges with the Strouhal number, coefficient of drag and separation angle as the mesh density increases, that is, as the number of elements in the direction of span increases. In the spanwise direction, Case G appears to be the optimum mesh with mesh density =0.1, as further increasing mesh density (Case F) has only a minor impact on separation angle, Strouhal number and drag coefficient. From results, it is also discovered that flow over cylinder at $Re= 3900$ is not just a 2-Dimensional analysis and that resolution in direction of span has a huge effect on the results. Changings in the spanwise domain length (L_z) and density of mesh (M_z) in direction of span are used in additional case studies. Additional case studies are then conducted, as shown in the table 4. For stable simulation, y^+ vale is smaller than unity is maintained in all case studies. From Case F and Case G, mesh density (M_z) of 0.05 and 0.1 respectively is used with a spanwise length (L_z) of 2D. Except for Case H, I and Case J, where the number of elements in the spanwise direction are much less and could not achieve minimum mesh density of 0.1, the results in these cases are well-converged. In order to gather the optimize results, elements number on circumference of cylinder (N_c) \times elements number on cylinder in radial flow direction (N_R) are 240 \times 60 respectively. Niaz [4] states that when the number of elements on the surface of cylinder is reduced from 240 and number of elements in radial direction (N_R) reduced from 60, it will results in Cd overprediction, a shorter length of recirculation, and a delay in angle of separation. Niaz [4] also states that the findings are unaffected by increasing N_c and N_R from 240 to 320 and 60 to 80, respectively. MA [26] and wissink and rodi [32] states that the spanwise resolution and domain are much important factors in predicting recirculation length accuracy. Breuer [9] and kravchenko and moin [31] states that, The size of domain in the spanwise plane is less contingent on outcomes if the density of mesh stays constant. The aim of this study is to see how spanwise length affected the numerical results. Further case studies (A to E and K to U) are also carried out with spanwise lengths (L_z) of 8D, 4D, πD , 2D, 0.5D, 0.1D with N_c and N_R of 240 and 60, respectively. From Case A and Case B, 8D spanwise length (L_z) was used using mesh density (M_z) of 0.1 and 0.2

respectively. Convergence in numerical results is obtained in Case A, which has N_T of 4.844×10^6 , L_z of $8D$ and mesh density of 0.1 . In Case A, recirculation length and separation angle are calculated to be 86.77 and 1.70 , respectively. These results agree well with Case G with the same mesh density (M_z), but smaller spanwise length of $2D$. Case B uses mesh densities of 0.2 , which results in a shorter length of recirculation and delay in angle of separation. In Case C, spanwise length of $4D$ is used, with $N_T \times 10^6$ of 2.5111 and mesh density $=0.1$. Similar results are obtained, and Case C numerical study matches well with Case A and Case G. In Case D and Case E, $N_T \times 10^6$ of 2.511 and 1.973 respectively, spanwise length of πD was used using mesh density of 0.07 and 0.1 respectively. Findings of both cases are quite similar, and it verifies that mesh density is much more important factor than spanwise resolution and spanwise length. From Case K to Case N, spanwise length of $1D$ was used using density of mesh ranging from 0.025 to 0.2 , matches well with the previous results with different spanwise lengths. From case Q to case T, spanwise length of $0.1D$ is used with varying density of mesh from 0.5 to 0.0125 . Results are satisfying even at $0.5D$ length and further increment of mesh density (case O and P) than 0.1 has very minor impact on results.

Case	$N_T \times 10^6$	L_z	N_z	$M_z = L_z / N_z$	$N_c \times N_R$	C_d	St	θ_s	L_r / D
F	2.5111	2D	40	0.05	240×60	0.98	0.201	87.66	1.70
G	1.316	2D	20	0.1	240×60	0.98	0.203	87.66	1.70
H	0.7181	2D	10	0.2	240×60	1.0424	0.201	89.19	1.36
I	0.4191	2D	5	0.4	240×60	1.2280	0.199	95.29	0.72
J	0.1798	2D	1	2	240×60	1.4204	0.195	104.4	0.38

Table 3: Results comparison with variation of grid in spanwise direction.

The results converge at a mesh density of 0.1 regardless of the spanwise domain length or total elements number and increasing the mesh density would only increase the computational cost and time. Also, these results of Cases A, C, E, G, M, Q with spanwise lengths $8D$, $4D$, πD , $2D$, $1D$, $0.5D$ respectively, with mesh density $=0.1$ in all cases, agrees well with the numerical results presented in table 4As a result, rather than concentrating on density of mesh (M_z) in the spanwise domain, spanwise length and near-field resolution of grids should take precedence. Recirculation length is the most sensitive parameter in calculating the numerical results. When it comes to measuring the recirculation length, there is some uncertainty in

numerical results. Parandeu [14] collected results with averaging time of 52 vortex shedding cycles and found a 10% uncertainty in results. Niaz [4] collected results with average time of 50 vortex shedding cycles. Wissink and Rodi [17, 32], Meyer [55] and Mani [54] collected results.

<i>Case</i>	$N_T \times 10^6$	L_z	N_z	$M_z = L_z / N_z$	$N_c \times N_R$	C_d	St	Θ_s	L_r / D
<i>A</i>	4.9033	8D	80	0.1	240×60	0.9878	0.143	87.66	1.7028
<i>B</i>	2.5111	8D	40	0.2	240×60	1.0300	0.21	89.19	1.42
<i>C</i>	2.5111	4D	40	0.1	240×60	0.9855	0.201	87.66	1.70
<i>D</i>	2.5111	π D	40	0.0785	240×60	0.9695	0.202	87.66	1.71
<i>E</i>	1.973	π D	31	0.1	240×60	0.9669	0.202	87.66	1.71
<i>F</i>	2.5111	2D	40	0.05	240×60	0.9781	0.197	87.66	1.70
<i>G</i>	1.316	2D	20	0.1	240×60	0.9787	0.203	87.66	1.7028
<i>H</i>	0.7181	2D	10	0.2	240×60	1.0424	0.201	89.19	1.3642
<i>I</i>	0.4191	2D	5	0.4	240×60	1.2280	0.199	95.29	0.7222
<i>J</i>	0.1798	2D	1	2	240×60	1.4204	0.198	104.44	0.3852
<i>K</i>	2.5111	1D	40	0.025	240×60	0.9995	0.212	87.66	1.60845
<i>L</i>	1.0171	1D	15	0.06	240×60	1.005	0.212	87.66	1.60845
<i>M</i>	0.7181	1D	10	0.1	240×60	1.0122	0.212	87.66	1.60845
<i>N</i>	0.4191	1D	5	0.2	240×60	1.1254	0.194	90.73	1.10505
<i>O</i>	2.5111	0.5D	40	0.0125	240×60	1.0424	0.205	87.66	1.42758
<i>P</i>	1.316	0.5D	20	0.025	240×60	1.0235	0.215	87.66	1.42758
<i>Q</i>	0.4191	0.5D	5	0.1	240×60	1.005	0.197	87.66	1.42758
<i>R</i>	0.3593	0.5D	4	0.125	240×60	1.0761	0.198	89.19	1.2594
<i>S</i>	0.2995	0.5D	3	0.166	240×60	1.0514	0.199	89.19	1.34192
<i>T</i>	0.179	0.5D	1	0.5	240×60	1.5975	0.198	101.3	0.3256
<i>U</i>	0.179	0.1D	1	0.1	240×60	1.7381	0.194	99.8	0.2516

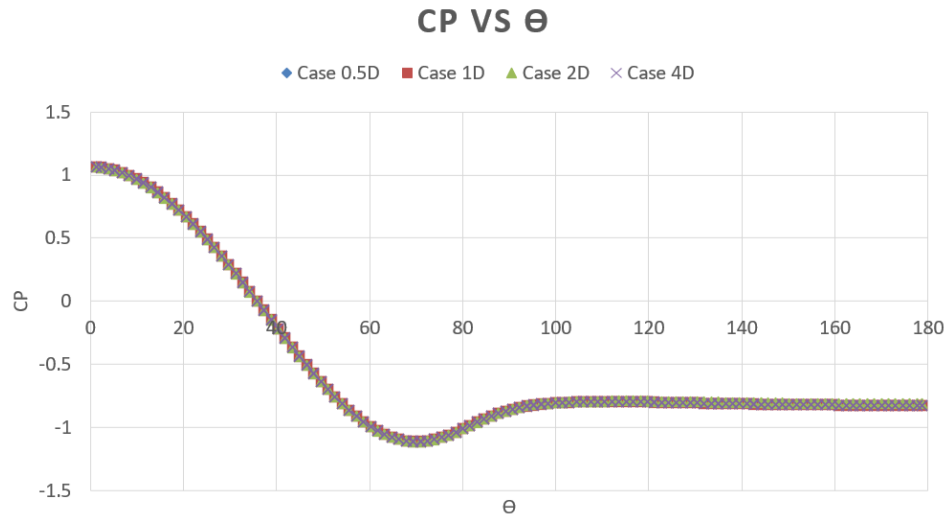
Table 4: Results comparison with variation of grid in spanwise direction.

around 60 vortex shedding cycles to come at their conclusions. Lysenko [12] collected results with averaging time of 150 vortex shedding cycles, necessary for fully developed flow. Franke and Frank [36] collected data from 200 vortex shedding cycles but were unable to calculate a convergent recirculation length value. The data in this study is collected over an averaging time of 120 vortex shedding cycles. The technique used (as discussed in section “Numerical model”) causes the recirculation length to converge. In addition to numerical and experimental studies, Table 5 shows the results of strouhal number, drag coefficient and length of recirculation in the present numerical studies (Case Q, Case M, and Case G, Case E, Case C, Case A). St and C_d values are in good agreement with the results of the other studies. The current numerical studies of this research are in good agreement with other experimental and numerical studies. The experimental results show the uncertainty in the recirculation length value (ranges from 1.19 to 1.56). While numerical results show uncertainty in recirculation length values (ranges from 1.02 to 1.64). The results indicates that the spanwise domain length has minimum and negligible impact on determining the length of recirculation for the spanwise length (L_z) of 0.5D, 1D, 2D, πD , 4D, 8D. From above results, it is concluded that 2D is the optimum spanwise length, as further increase in spanwise length did not change results and only increase computational cost and time for simulations. The present numerical results are more similar to experimental results of parnaudeau [14] and numerical results of franke [36], Dong [15], Lysenko [12], afgan [50] and Niaz Bahadur [4]. In terms of angle of separation, the majority of other numerical studies result in separation delay, expect Niaz Bahadur [4]. This present numerical analysis accurately captured the angle of separation point, which is similar to numerical results of Niaz Bahadur [4].

<i>Case</i>	<i>C_d</i>	<i>θ_s</i>	<i>Lr/D</i>	<i>St</i>
[2], <i>experiment</i>	0.98±0.005	---	1.33±0.2	0.215±0.005
[14], <i>experiment</i>	---	---	1.560.21	0.21
<i>Laurenco and shih, experiment</i>	0.99	86	1.19	0.22
[18], <i>experiment</i>	0.98±0.005	---	---	0.21
[15], <i>DNS</i>	---	---	1.47	0.203
[57]	0.88	911	1.04	0.250
[12], <i>LES</i>	0.97	89	1.67	0.209
[11], <i>LES</i>	1.15	86.5	1.02	0.215
[50], <i>LES</i>	1.02	86	1.49	0.207
[58], <i>LES</i>	0.99	---	1.37	0.212
[4], <i>Case D, LES</i>	0.98	86.18	1.68	0.218
[4], <i>Case L, LES</i>	0.986	86.18	1.70	0.205
[4], <i>Case O, LES</i>	0.982	86.18	1.73	0.21
<i>Present Case A, 8D, LES</i>	0.987	86.77	1.70	0.205
<i>Present Case C, 4D, LES</i>	0.985	86.77	1.70	0.201
<i>Present Case E, πD, LES</i>	0.97	86.77	1.71	0.202
<i>Present Case G, 2D, LES</i>	0.98	86.77	1.70	0.203
<i>Present Case M, 1D, LES</i>	1.01	86.77	1.608	0.212
<i>Present Case Q, 0.5D, LES</i>	1.005	86.77	1.427	0.204

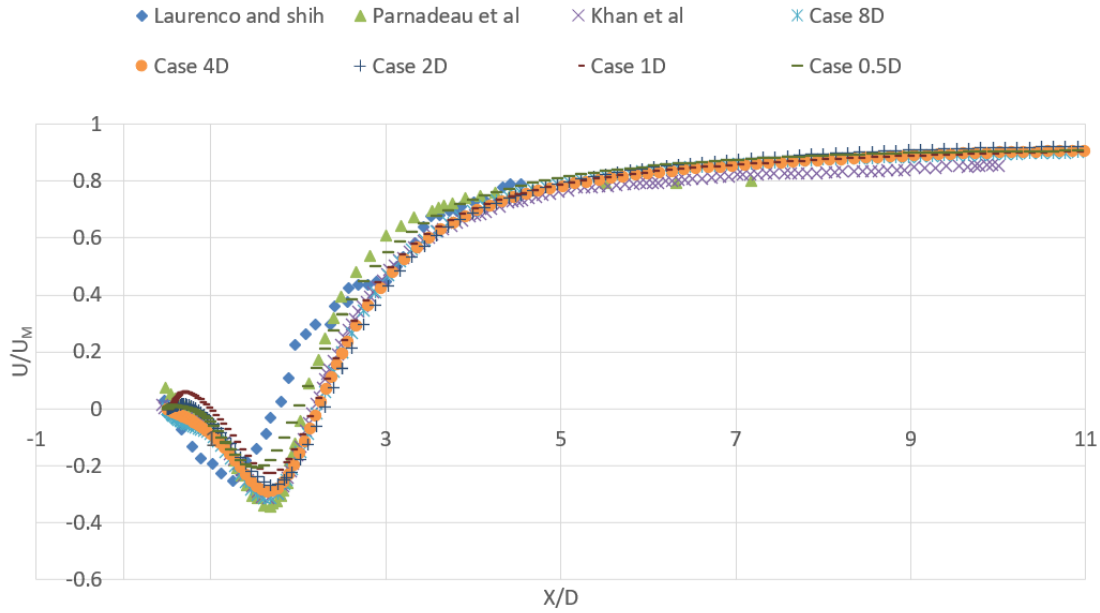
Table 5: At Re=3900 Comparison between numerical and experimental results.

Graph 1 depicts the distribution of pressure over the surface of cylinder, together with the numerical results of Niaz Bahadur [4] at Re=3900 and experimental results of Norberg [2] at Re=4020. This research demonstrates that findings are in strong accordance with the numerical and experimental results.



Graph 1: Coefficient of pressure (C_p) vs Angle (Θ)

The mean streamwise velocity profiles in the wake of the cylinder are shown in graph 2. The mean velocity is calculated from the cylinder's centerline to a 10-diameter distance away from the cylinder, as shown in the Figure 5. The results show that the detached eddy simulation (DES) has a slightly shorter recirculation length in comparison with experimental results. There is a small disparity between the experimental results and the findings of this research study. This disparity may be due to Lourenco and Shih's usage of the PIV process, where an external disruption causes the separating shear layer to transition early [31]. Overall, this research study validates previous numerical and experimental results. This LES case study's recirculation length matches well with Niaz Bahadur [4] numerical results.



Graph 2: Mean stream velocity profile at centerline, behind the cylinder.

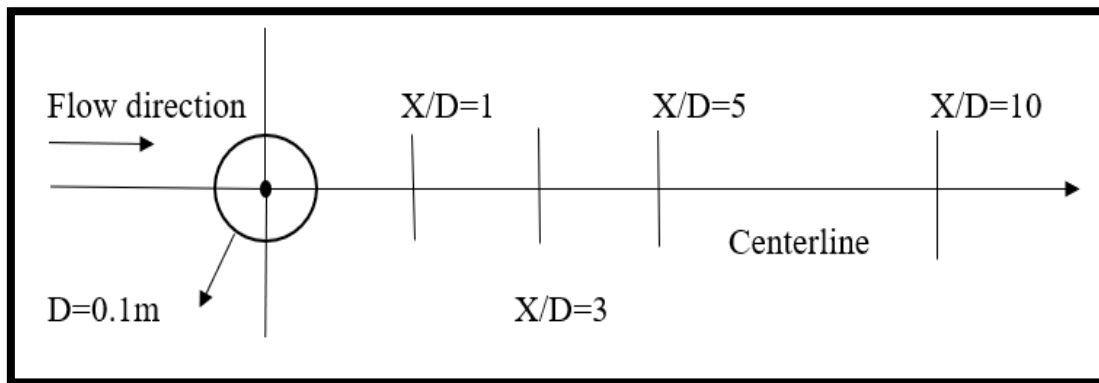
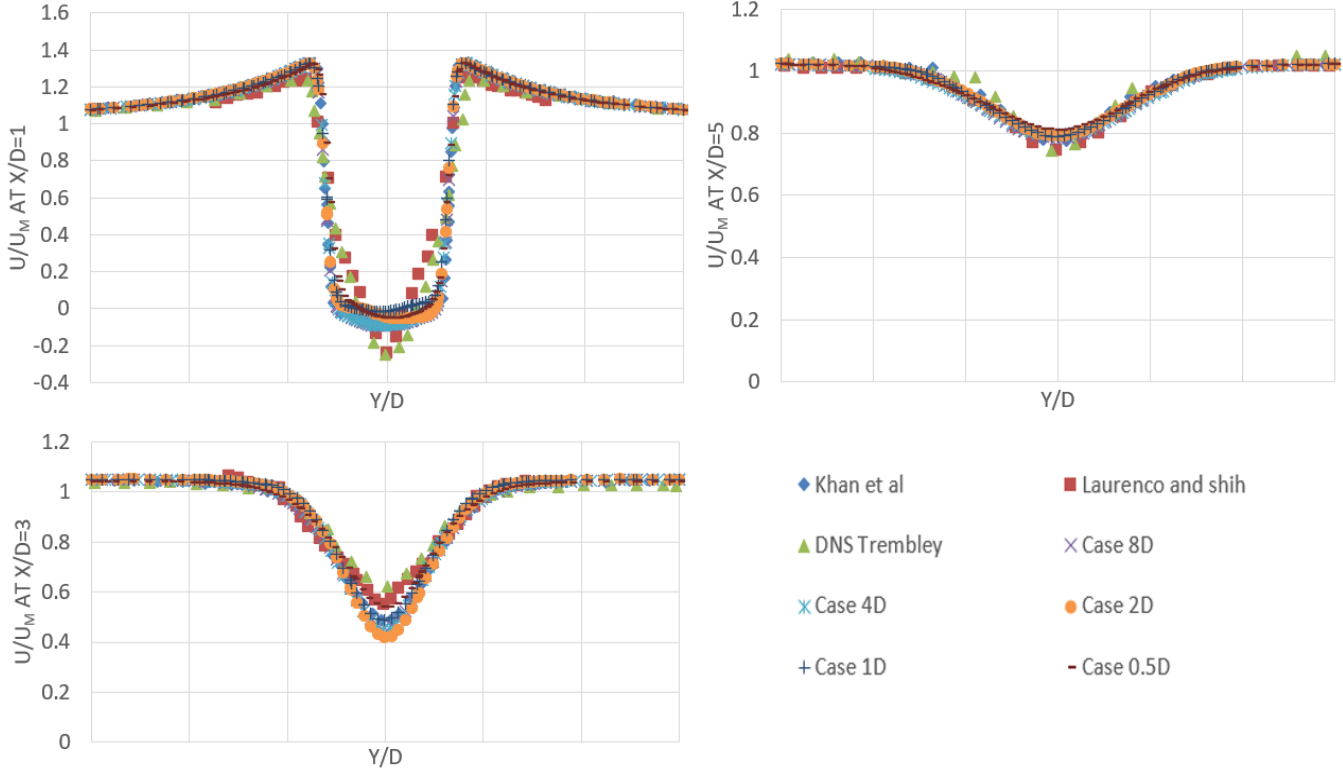


Figure 5: Vertical profiles and centerline sketch behind the cylinder.

Graph 3 compares the mean streamwise velocity profiles in the wake area to previous studies (at distances $x/D=1$, $x/D=3$ and $x/D=5$). The data ranges from $y/d= -3$ to $y/d= 3$. Dividing the mean velocity in streamwise by the inlet velocity, the mean streamwise velocity is normalized. Present results agrees well with Niaz bahadur[4] results. Also, there is a slight difference in peak at $x/d=1$, this discrepancy might be attributable to Lourenco and Shih's different experimental methods, where some external disruption will

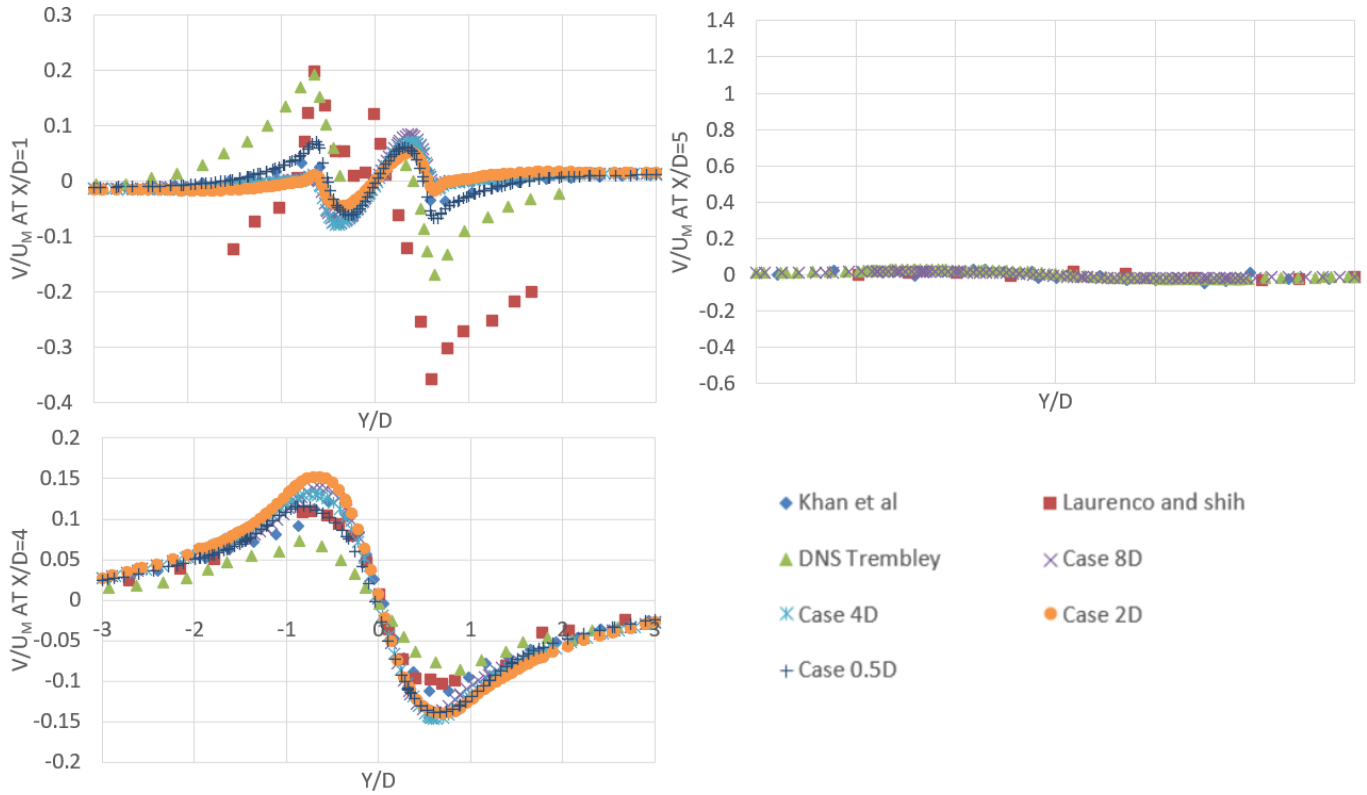
cause early transition and shear layers separation. At $X/D=1$, a U-shape profile is observed, indicating that the current data are reliable and accurate. When resolution of grids are not enough fine in the spanwise domain, a V-shaped profile is observed, according to Niaz Bahadur [4] and Kravchenko and Moin [31].



Graph 3: Comparison of mean stream velocity profiles of flow over cylinder at $X/D=1$ for present study and other numerical and experimental results.

At distances $x/D= 1$, $x/D= 3$ and $x/D= 5$, the mean crossflow velocity profiles in the wake region is shown in graphs 4. There is a difference between present study results and Lourenco's and Shih's experimental and Trembley [11] results in the wake region near the cylinder at $x/D=1$. However, the current LES study is in accordance with the mean crossflow velocity component profiles by Niaz Bahadur [4]. This LES analysis captures the results well, away from the cylinder. Norberg [2] investigated the wake flow near a cylinder with various geometrical parameters and found that the boundary condition in the spanwise domain has a major impact on the onset shear layer instability. The periodic condition at boundaries is used in

simulations in the spanwise faces, so the aspect ratio has no effect on the results near the cylinder. However, near the wake, a grid independence analysis is needed to obtain accurate results.



Graph 4: Comparison of mean crossflow velocity profiles of flow over cylinder at $X/D=3$ for present study and other numerical and experimental results.

CHAPTER 5: Conclusions

At Reynolds number 3900, the flow over a cylinder was simulated using the Large Eddy Simulation (LES) model. In comparison to other numerical and experimental studies, Strouhal number, drag coefficient and separation angle are all very well captured. 2D spanwise length considered as optimum spanwise length as further increase in spanwise length only increases computational cost and time and did not influence on numerical results and recirculation length is very small, when spanwise length decreases than 2D (in 0.5D and 1D). Recirculation length is the most sensitive parameter in gathering all numerical results. Mesh with mesh density=0.1 considered as optimum mesh design. Mesh density < 0.1 results are same as with mesh density =0.1. In addition, coarse mesh (mesh density > 0.1) in the spanwise direction results in an overestimated drag (C_d) value, shorter recirculation value (L_r/D), a delay in the angle of separation (Θ_s), underestimated value of Strouhal number (S_t), according to this research. The findings of this analysis are in line with the experimental findings, and a better profile is predicted than other numerical simulations. The mesh density in the spanwise direction has a significant impact on the results of numerical simulations, whereas experimental research indicate that the aspect ratio considerably influences the results in the wake near to cylinder. The instantaneous field from static flow with k- ω models is used for LES run as an initial field which reduces the simulation time in obtaining convergent statistical results.

Future Recommendations

In this project, we found that mesh resolution in spanwise direction plays important role for better quality results. This study was performed on circular fixed cylinder. This study could be further expanded by utilizing different shapes of cylinders (triangular, rectangular, square). This study also performs with increasing number of cylinders.

The findings of this study will be beneficial to practitioners and decision makers in the field of Computational fluid dynamics and aerodynamics for better understanding the nature of wake and flow assessment techniques as well to optimize computational time and cost before going into physical experiments.

References

1. Beaudan, P. and P. Moin, *Numerical experiments on the flow past a circular cylinder at sub-critical Reynolds number*. 1994, Stanford Univ CA Thermosciences Div.
2. Norberg, C., *Effects of Reynolds number and a low-intensity freestream turbulence on the flow around a circular cylinder*. Chalmers University, Goteborg, Sweden, Technological Publications, 1987. **87**(2): p. 1-55.
3. Khan, N.B. and Z. Ibrahim, *Numerical investigation of vortex-induced vibration of an elastically mounted circular cylinder with One-degree of freedom at high Reynolds number using different turbulent models*. Proceedings of the Institution of Mechanical Engineers, Part M: Journal of Engineering for the Maritime Environment, 2019. **233**(2): p. 443-453.
4. Khan, N.B., et al., *Numerical investigation of flow around cylinder at Reynolds number= 3900 with large eddy simulation technique: effect of spanwise length and mesh resolution*. Proceedings of the Institution of Mechanical Engineers, Part M: Journal of Engineering for the Maritime Environment, 2019. **233**(2): p. 417-427.
5. Khan, N.B., et al., *Numerical investigation of the vortex-induced vibration of an elastically mounted circular cylinder at high Reynolds number ($Re= 104$) and low mass ratio using the RANS code*. Plos One, 2017. **12**(10): p. e0185832.
6. Khan, N.B., et al., *Numerical simulation of flow with large eddy simulation at $Re= 3900$: A study on the accuracy of statistical quantities*. International Journal of Numerical Methods for Heat & Fluid Flow, 2019.
7. Williamson, C.H., *Vortex dynamics in the cylinder wake*. Annual review of fluid mechanics, 1996. **28**(1): p. 477-539.
8. Bearman, P., *Circular cylinder wakes and vortex-induced vibrations*. Journal of Fluids and Structures, 2011. **27**(5-6): p. 648-658.
9. Breuer, M., *Large eddy simulation of the subcritical flow past a circular cylinder: numerical and modeling aspects*. International journal for numerical methods in fluids, 1998. **28**(9): p. 1281-1302.
10. Sarpkaya, T., *A critical review of the intrinsic nature of vortex-induced vibrations*. Journal of fluids and structures, 2004. **19**(4): p. 389-447.
11. Tremblay, F., M. Manhart, and R. Friedrich, *LES of flow around a circular cylinder at a subcritical Reynolds number with cartesian grids*, in *Advances in LES of Complex flows*. 2002, Springer. p. 133-150.
12. Lysenko, D.A., I.S. Ertesvåg, and K.E. Rian, *Large-eddy simulation of the flow over a circular cylinder at Reynolds number 3900 using the OpenFOAM toolbox*. Flow, turbulence and combustion, 2012. **89**(4): p. 491-518.
13. Lysenko, D.A., I.S. Ertesvåg, and K.E. Rian, *Large-eddy simulation of the flow over a circular cylinder at Reynolds number 2×10^4* . Flow, turbulence and combustion, 2014. **92**(3): p. 673-698.
14. Parnaudeau, P., et al., *Experimental and numerical studies of the flow over a circular cylinder at Reynolds number 3900*. Physics of Fluids, 2008. **20**(8): p. 085101.
15. Dong, S., et al., *A combined direct numerical simulation-particle image velocimetry study of the turbulent near wake*. Journal of Fluid Mechanics, 2006. **569**: p. 185.

16. Norberg, C., *An experimental investigation of the flow around a circular cylinder: influence of aspect ratio*. Journal of Fluid Mechanics, 1994. **258**: p. 287-316.
17. Wissink, J.G. and W. Rodi, *Large-scale computations of flow around a circular cylinder*, in *High performance computing on vector systems 2007*. 2008, Springer. p. 71-81.
18. Ong, L. and J. Wallace, *The velocity field of the turbulent very near wake of a circular cylinder*. Experiments in fluids, 1996. **20**(6): p. 441-453.
19. Zhao, M., et al., *Three-dimensional numerical simulation of vortex-induced vibration of an elastically mounted rigid circular cylinder in steady current*. Journal of Fluids and Structures, 2014. **50**: p. 292-311.
20. Khalak, A. and C. Williamson, *Dynamics of a hydroelastic cylinder with very low mass and damping*. Journal of Fluids and Structures, 1996. **10**(5): p. 455-472.
21. Guilmineau, E. and P. Queutey, *Numerical simulation of vortex-induced vibration of a circular cylinder with low mass-damping in a turbulent flow*. Journal of fluids and structures, 2004. **19**(4): p. 449-466.
22. Pan, Z., W. Cui, and Q. Miao, *Numerical simulation of vortex-induced vibration of a circular cylinder at low mass-damping using RANS code*. Journal of Fluids and Structures, 2007. **23**(1): p. 23-37.
23. Hover, F., S. Miller, and M. Triantafyllou, *Vortex-induced vibration of marine cables: experiments using force feedback*. Journal of fluids and structures, 1997. **11**(3): p. 307-326.
24. Nguyen, V.-T. and H.H. Nguyen, *Detached eddy simulations of flow induced vibrations of circular cylinders at high Reynolds numbers*. Journal of Fluids and Structures, 2016. **63**: p. 103-119.
25. Williamson, C. and R. Govardhan, *Vortex-induced vibrations*. Annu. Rev. Fluid Mech., 2004. **36**: p. 413-455.
26. MA, X., G.-S. Karamanos, and G. Karniadakis, *Dynamics and low-dimensionality of a turbulent near wake*. Journal of fluid mechanics, 2000. **410**: p. 29-65.
27. Ramzi, N., et al. *Experimental analysis on vortex-induced vibration of a rigid cylinder with different surface roughness*. in *IOP Conference Series: Materials Science and Engineering*. 2019. IOP Publishing.
28. Rajani, B., A. Kandasamy, and S. Majumdar, *On the reliability of eddy viscosity based turbulence models in predicting turbulent flow past a circular cylinder using URANS approach*. 2012.
29. Zhang, H., et al., *Large-eddy simulation of the flow past both finite and infinite circular cylinders at $Re = 3900$* . Journal of Hydrodynamics, 2015. **27**(2): p. 195-203.
30. Fröhlich, J., et al., *Large eddy simulation of flow around circular cylinders on structured and unstructured grids*, in *Numerical flow simulation I*. 1998, Springer. p. 319-338.
31. Kravchenko, A.G. and P. Moin, *Numerical studies of flow over a circular cylinder at $Re D = 3900$* . Physics of fluids, 2000. **12**(2): p. 403-417.
32. Wissink, J. and W. Rodi, *Numerical study of the near wake of a circular cylinder*. International journal of heat and fluid flow, 2008. **29**(4): p. 1060-1070.
33. Townsend, A., *The fully developed wake of a circular cylinder*. Australian Journal of Chemistry, 1949. **2**(4): p. 451-468.
34. Yamada, H., et al., *Turbulence measurements in a two-dimensional turbulent wake*. Yamaguchi University, Technology Reports, 1980. **2**: p. 329-339.
35. Norberg, C., *Fluctuating lift on a circular cylinder: review and new measurements*. Journal of Fluids and Structures, 2003. **17**(1): p. 57-96.

36. Franke, J. and W. Frank, *Large eddy simulation of the flow past a circular cylinder at $ReD= 3900$* . Journal of wind engineering and industrial aerodynamics, 2002. **90**(10): p. 1191-1206.
37. Shao, J. and C. Zhang, *Numerical analysis of the flow around a circular cylinder using RANS and LES*. International Journal of Computational Fluid Dynamics, 2006. **20**(5): p. 301-307.
38. Young, M. and A. Ooi, *Comparative assessment of LES and URANS for flow over a cylinder at a Reynolds number of 3900*. 2007.
39. Feng, Z., et al. *Comparisons of Subgrid-Scale Models for OpenFoam Large-Eddy Simulation*. in *Journal of Physics: Conference Series*. 2021. IOP Publishing.
40. Sircar, A., et al., *Turbulent flow and heat flux analysis from validated large eddy simulations of flow past a heated cylinder in the near wake region*. Physics of Fluids, 2020. **32**(12): p. 125119.
41. Liu, H. *Large eddy simulation of flow past a 3D cylinder at $Re= 3900$* . in *IOP Conference Series: Materials Science and Engineering*. 2018. IOP Publishing.
42. Hinze, J.O., *Experimental investigation on secondary currents in the turbulent flow through a straight conduit*. Applied Scientific Research, 1973. **28**(1): p. 453-465.
43. Smagorinsky, J., *General circulation experiments with the primitive equations: I. The basic experiment*. Monthly weather review, 1963. **91**(3): p. 99-164.
44. Lilly, D.K., *A proposed modification of the Germano subgrid-scale closure method*. Physics of Fluids A: Fluid Dynamics, 1992. **4**(3): p. 633-635.
45. Germano, M., et al., *A dynamic subgrid-scale eddy viscosity model*. Physics of Fluids A: Fluid Dynamics, 1991. **3**(7): p. 1760-1765.
46. Ferziger, J.H., M. Perić, and R.L. Street, *Computational methods for fluid dynamics*. Vol. 3. 2002: Springer.
47. Menter, F.R., *Two-equation eddy-viscosity turbulence models for engineering applications*. AIAA journal, 1994. **32**(8): p. 1598-1605.
48. Greifzu, F., et al., *Assessment of particle-tracking models for dispersed particle-laden flows implemented in OpenFOAM and ANSYS FLUENT*. Engineering Applications of Computational Fluid Mechanics, 2016. **10**(1): p. 30-43.
49. Fang, Y.Y. and Z.L. Han. *Numerical experimental research on the hydrodynamic performance of flow around a three dimensional circular cylinder*. in *Applied Mechanics and Materials*. 2011. Trans Tech Publ.
50. Afgan, I., et al., *Large eddy simulation of the flow around single and two side-by-side cylinders at subcritical Reynolds numbers*. Physics of Fluids, 2011. **23**(7): p. 075101.
51. Mittal, S., *Free vibrations of a cylinder: 3-D computations at $Re= 1000$* . Journal of Fluids and Structures, 2013. **41**: p. 109-118.
52. Zdravkovich, M., *Conceptual overview of laminar and turbulent flows past smooth and rough circular cylinders*. Journal of wind engineering and industrial aerodynamics, 1990. **33**(1-2): p. 53-62.
53. Prsic, M.A., et al., *Large Eddy Simulations of flow around a smooth circular cylinder in a uniform current in the subcritical flow regime*. Ocean engineering, 2014. **77**: p. 61-73.
54. Mani, A., P. Moin, and M. Wang, *Computational study of optical distortions by separated shear layers and turbulent wakes*. Journal of fluid mechanics, 2009. **625**: p. 273.
55. Meyer, M., S. Hickel, and N. Adams, *Assessment of implicit large-eddy simulation with a conservative immersed interface method for turbulent cylinder flow*. International Journal of Heat and Fluid Flow, 2010. **31**(3): p. 368-377.
56. Heggernes, K.K., *Numerical simulation of three-dimensional viscous flow around marine structures*. 2005.

57. Liaw, K.F., *Simulation of flow around bluff bodies and bridge deck sections using CFD*. 2005, University of Nottingham Nottingham.
58. Park, N., et al., *A dynamic subgrid-scale eddy viscosity model with a global model coefficient*. *Physics of Fluids*, 2006. **18**(12): p. 125109.